Chinese Journal of Chemical Engineering 67 (2024) 238–246

Contents lists available at ScienceDirect

Chinese Journal of Chemical Engineering

journal homepage: www.elsevier.com/locate/CJChE

Full Length Article

# Lipase and photodecarboxylase coexpression: A potential strategy for alkane-based biodiesel production from natural triglycerides

Yong-Yi Zeng [1], Xin-Yi Xu [1], Jin-Xuan Xie [1], Wen-Li Chen [1], Lan Liu [1, 2], Xin-Jian Yin [1, *], Bi-Shuang Chen [1, 2, *]

[1] School of Marine Sciences, Sun Yat-Sen University, Zhuhai 519080, China
[2] Southern Marine Science and Engineering Guangdong Laboratory (Zhuhai), Zhuhai 519080, China

ARTICLE INFO

*Article history:*
Received 7 August 2023
Received in revised form
15 November 2023
Accepted 15 November 2023
Available online 8 December 2023

*Keywords:*
Alkane-based biodiesel
Renewable biomass
Co-overexpression
Lipase
Photodecarboxylase

ABSTRACT

Alkane-based biodiesel is considered the next generation of biodiesel owing to its potential environmental benefits and the fact that it exhibits much higher specific caloric values than traditional biodiesel. However, the formidable obstacle impeding the commercialization of this cutting-edge fuel alternative lies in the cost associated with its production. In this study, an engineered strain *Escherichia coli* (*E. coli*) showcasing harmonized coexpression of a lipase (from *Thermomyces lanuginosus lipase*, *TLL*) and a fatty acid photodecarboxylase (from *Chlorella variabilis*, *Cv*FAP) was first constructed to transform triglycerides into alkanes. The potential of *E. coli* BL21 (DE3)/pRSFDuet-1-*TLL*-*Cv*FAP for alkane synthesis was evaluated with tripalmitin as a model substrate under various process conditions. Following a comprehensive examination of the reaction parameters, the scope of the biotransformation was expanded to 'real' substrates (vegetable oils). The results showed that bioderived oils can be transformed into alkanes with high yields (0.80–10.20 mmol·L$^{-1}$) under mild conditions (35 °C, pH 8.0, and 36 h) and blue light illumination. The selected processes were performed on an increased lab scale (up to 100 ml) with up to 24.77 mmol·L$^{-1}$ tripalmitin, leading to a yield of 18.89 mmol·L$^{-1}$ pentadecane. With the employment of a method for efficiently producing alkanes under mild conditions and a simple procedure to isolate alkanes from the reaction system, the utilization of sustainable biomass as a fundamental feedstock emerges as the primary solution to lower the cost of alkane-based biodiesel. Thus, this study proposes a readily implementable and highly effective approach for alkane-based biodiesel production.


## 1. Introduction

The ever-increasing consumption of nonrenewable fossil fuels and the environmental issues raised during their development and application processes present a challenge [1]. A renewable and environmentally viable fuel such as biodiesel seems to be a solution to this challenge. The term "biodiesel" usually denotes fatty acid methyl esters (FAMEs) and fatty acid ethyl esters (FAEEs), which can be produced *via* different reactions with different types of catalysts [2]. Among all methods for producing biodiesel (direct use and blending, microemulsions, thermal cracking, and transesterification) [3], the (*trans*)esterification of vegetable oils, animal fats, waste oils, *etc*. with methanol or ethanol has been a research focus for decades and has already been applied worldwide [4–6].

However, the reversible (*trans*)esterification procedure inevitably encounters equilibrium issues [7,8]. On the one hand, significant molar surpluses of alcohols are required to achieve near-full conversion, which leads to harsh operating conditions and high energy consumption. On the other hand, the byproduct (water) challenges the practicability of this approach, leading to saponification and catalyst inactivation. Moreover, FAMEs and FAEEs are not equal to the composition of fossil fuel and therefore can only be mixed with petrochemical diesel at a ratio of less than 20% [9,10]. As a result, transforming vegetable oils/animal fats/waste oils into alkanes *via* hydrolysis and decarboxylation instead of esterification could be an interesting alternative

* Corresponding authors. Tel.: +86 0756 3668775 (B.-S. Chen).
*E-mail addresses:* yinxj5@mail.sysu.edu.cn (X.-J. Yin), chenbsh23@mail.sysu.edu.cn (B.-S. Chen).

https://doi.org/10.1016/j.cjche.2023.11.013
1004-9541/

strategy. Alkane-based biodiesel is generally denoted as the next generation of biodiesel.

Triglycerides (and free fatty acids as the balance substances) are the main components of natural oils and can be converted into fatty acids by cleaving the ester functions. The challenging step is the decarboxylation of fatty acids into the corresponding $C_1$-shortened alkanes [11]. The established chemical catalytic systems usually require harsh conditions, leading to poor energy efficiency. In addition, the production of alkanes is hampered by the uncontrollable reactivity of radical intermediates (low selectivity of this reaction), necessitating high $H_2$ pressure to inhibit side reactions [12]. Interestingly, fatty acid photodecarboxylases (FAPs) from microalgae can catalyze the photocatalytic decarboxylation of fatty acids under mild conditions without typical radical byproducts [13–16], owing to the confinement of the alkyl radical in the enzyme's active site [17]. Therefore, an enzymatic method combining a lipase and a photodecarboxylase to transform natural triglycerides into alkanes has recently been highlighted as an eco-friendly and energy-saving approach for alkane-based biodiesel production.

Although the reaction system benefits from its simplicity and excellent efficiency, few protocols have been developed thus far. One of the pioneering works was conducted by Hollmann and coworkers [7], who proposed a nonenzymatic cascade comprising a lipase from *Candida rugosa* (*Cr*Lip) and a photodecarboxylase from *Chlorella variabilis* NC64A (*Cv*FAP). The starting material, triolein, is hydrolyzed by *Cr*Lip to free oleic acid, which is subsequently decarboxylated by *Cv*FAP into the corresponding heptadecane with a good overall yield. Wang *et al.* [8] expanded the scope of cascade reactions to a series of vegetable oils and waste cooking oil. Meanwhile, the Wang group [18] also established a lipase-photodecarboxylase multienzyme complex based on the SpyTag/SpyCatcher self-assembly strategy. The efficiency of alkane synthesis is significantly improved compared to double-free enzyme catalysis. However, poor substrate transport efficiency is a major issue for multienzyme complexes, causing low reaction rates [19]. One of the solutions to this issue is coexpressing the two enzymes in a host strain to construct a two-enzyme cascade catalytic reaction for the efficient production of biodiesel [20,21].

Herein, we aim to thoroughly design a cascade biosynthesis system in *Escherichia coli* BL21 (DE3) by coexpressing a lipase and a photodecarboxylase for alkane production using renewable biomass as the raw material. The efficiency of the bienzyme-coordinated expression system, the use of renewable resources, easy scalability, and compatibility with a rather broad scope of natural oils significantly contribute to the production of alkane-based biodiesel.

## 2. Materials and Methods

### 2.1. Reagent and detection

Competent *E. coli* BL21 (DE3), *E. coli* Trans 5α, and the vectors pET28a(+), pACYCDuet-1, and pRSFDuet-1 were purchased from Tsingke Biotechnology Co., Ltd. (Beijing, China), MiaoLing Plasmid Platform (Hubei, China), and HedgehogBio Science and Technology Ltd. (Shanghai, China). All the chemicals and solvents were purchased from Macklin, Aladdin, or TCI and were of analytical grade or higher, unless otherwise specified.

Hydrolysis and photodecarboxylation reactions occurred simultaneously under blue light exposure. After a reaction for 36 h, the alkanes were extracted from two times the volume of ethyl acetate, according to previous work [16]. The resulting alkanes were identified by gas chromatography (GC). The GC analyses were performed with a Scion GC 456 system equipped with a flame ionization detector (FID) and Agilent J&W GC columns (60 m × 0.53 mm × 2.5 μm) using $N_2$ as the carrier gas. The following conditions were used for alkane separation: injector 260 °C, detector (FID) 280 °C, FID hydrogen 30 and oxygen 300, column flow 20 $ml \cdot min^{-1}$, temperature program: start 110 °C, hold time 2 min; rate 25 $°C \cdot min^{-1}$ to 190 °C, hold time 2 min; rate 30 $°C \cdot min^{-1}$ to 280 °C, hold time 5 min; rate 30 $°C \cdot min^{-1}$ to 310 °C, hold time 2 min. The peaks of the respective alkanes were identified using standard alkanes. The retention times were as follows: pentadecane = 9.50 min, heptadecane = 10.99 min.

### 2.2. Plasmid construction

#### 2.2.1. Construction of the pACYCDuet-TLL-CvFAP and pRSFDuet-TLL-CvFAP coexpression plasmids

pACYCDuet-1 and pRSFDuet-1 are two commercial protein dual expression vectors with identical cloning/expression regions; therefore, these two coexpression strains were constructed in the same way. The pRSFDuet-*TL*L plasmid was first used as a template to amplify the *TL*L gene fragment using P1 (ACYC-1-*TL*L-F) and P2 (ACYC-1-*TL*L-R) (Table S2) as the primer pairs. The pACYCDuet-1 (or pRSFDuet-1) empty plasmid was used as a template, and BamHI and EcoRI were selected for double digestion to obtain the linearized vector fragment. The *TL*L gene fragment was cloned into the first multiple cloning sites of the Duet plasmid by a recombination reaction to obtain the Duet-*TL*L recombinant plasmid. The pET28a-*Cv*FAP recombinant plasmid was then used as a template to amplify the *Cv*FAP gene fragment using P3 (ACYC-2-*Cv*FAP-F) and P4 (ACYC-2-*Cv*FAP-R) [or P5 (RSF-2-*Cv*FAP-F) and P6 (RSF-2-*Cv*FAP-R)] as the primer pairs (Table S2). The Duet-*TL*L recombinant plasmid was used as a template to obtain the linearized vector fragment by double digestion, with HindIII and NotI selected as the digestion sites. The *Cv*FAP gene fragment was cloned into the second polyclonal site of the Duet plasmid by recombination to obtain the pACYCDuet-*TLL*-*Cv*FAP and pRSFDuet-*TLL*-*Cv*FAP coexpression plasmids.

#### 2.2.2. Construction of the pET28a-CvFAP-SD-TLL coexpression plasmid

The linearized long fragment was obtained by double digestion with HindIII and NotI using the pET28a-*Cv*FAP recombinant plasmid as a template. A short-linearized fragment was amplified using pET28a-*TL*L as a template and P11 (SD-*TL*L-MB-F) and P12 (SD-*TL*L-MB-R) as primer pairs (Table S2). The two fragments were ligated by recombination reactions to obtain the pET28a-*Cv*FAP-SD-*TL*L coexpression plasmid.

#### 2.2.3. Construction of the pET28a-(DualTer)-CvFAP-TLL coexpression plasmid

The linearized long fragment was obtained by double digestion with NdeI and EcoRI using the pET28a(+) empty vector as a template. A short-linearized fragment was amplified using pET28a-*TL*L as a template and P7 (T7T-*TL*L-F) and P8 (T7T-*TL*L-R) as primers (Table S2). The two fragments were ligated by recombination reactions to obtain the pET28a-Ter-*TL*L plasmid. Next, the linearized long fragment was obtained by double digestion with HindIII and XhoI using the pET28a-Ter-*TL*L recombinant plasmid as a template. The linearized short fragment was amplified using pET28a-*Cv*FAP as the template and P9 (T7T-*Cv*FAP-F) and P10 (T7T-*Cv*FAP-R) as the primer pairs (Table S2). The two fragments were ligated by recombination reactions to obtain the pET28a-(DualTer)-*Cv*FAP-*TL*L recombinant plasmid.

### 2.3. Preparation of whole cells of E. coli BL21 (DE3)/pRSFDuet-1-TLL-CvFAP)

Recombinant *E. coli* BL21 (DE3) strains containing the recombinant coexpression plasmid *TLL-Cv*FAP were cultured in Terrific Broth (TB) medium containing 50 $\mu g \cdot ml^{-1}$ kanamycin (using chloramphenicol only on the pACYCDuet-1 vector) at 37 °C. When the $OD_{600}$ values reached 0.7–0.8, the production of the recombinant protein was induced by the addition of isopropyl thio-β-D-galactoside (IPTG) to a final concentration of 0.5 $mmol \cdot L^{-1}$. Cultures were grown after induction at 18 °C for 18 h. An *E. coli* pET28a(+) empty vector was cultivated and induced with the same system as a control experiment. Cells were harvested by centrifugation (11000 × *g*, 10 min, 4 °C) and washed two times with Tris-HCl buffer (pH 8.0, 50 $mmol \cdot L^{-1}$, NaCl, 100 $mmol \cdot L^{-1}$). After storing the harvest in aliquots at −20 °C, aliquots of 0.0500 g were transferred to clean and dry Eppendorf micro test tubes (EP tubes).

### 2.4. General procedure for hydrolytic photodecarboxylation

Reactions were performed in 5-ml screw-capped glass vials to prevent the evaporation of the substrate/product. For tripalmitin, the reaction conditions were as follows: 1000 μl of Tris-HCl buffer (pH 8.0, 100 $mmol \cdot L^{-1}$) containing 0.0500 g *E. coli* BL21 (DE3)/pRSFDuet-1-*TLL-Cv*FAP was added to a transparent glass vial (total reaction volume was 1 ml). For the blank reaction, the setup was the same, but heat-denaturized cells and heat-denaturized cell-free extract (99 °C, 10 min) were used. The final conditions of this reaction were [*E. coli* BL21 (DE3)/pRSFDuet-1-*TLL-Cv*FAP] = 0.0500 $g \cdot ml^{-1}$, [tripalmitin] = 24.77 $mmol \cdot L^{-1}$, exposed under blue light, and stirred at 250 $r \cdot min^{-1}$ for 36 h.

For natural oils, the reaction conditions were as follows: 950 μl of Tris-HCl buffer (pH 8.0, 100 $mmol \cdot L^{-1}$) containing 0.0500 g of *E. coli* BL21 (DE3)/pRSFDuet-1-*TLL-Cv*FAP and 50 μl of oil were added to a transparent glass vial (total reaction volume was 1 ml). For the blank reaction, the setup was the same, but heat-denaturized cells and heat-denaturized cell-free extract (99 °C, 10 min) were used. The final conditions of this reaction were [*E. coli* BL21 (DE3)/pRSFDuet-1-*TLL-Cv*FAP] = 0.0500 $g \cdot ml^{-1}$, [Oil] = 50 $\mu l \cdot ml^{-1}$, exposed under blue light, and stirred at 250 $r \cdot min^{-1}$ for 36 h. The yields of products were quantified by Gas Chromatography (GC) using a calibration line. Experiments were performed in triplicate, and the average values were shown as the final results.

### 2.5. Reaction time course monitoring

Reactions were carried out as described in the general procedure for hydrolytic photodecarboxylation using tripalmitin (24.77 $mmol \cdot L^{-1}$). The reaction was carried out for 72 h, and samples were taken at 3, 6, 12, 24, 48, and 72 h for detection. After extraction with ethyl acetate (2 × 0.5 ml), samples were analyzed by GC for yield determination.

### 2.6. Investigation of pH values and thermostability

*E. coli* BL21 (DE3)/pRSFDuet-1-*TLL-Cv*FAP was incubated at different temperatures (30–70 °C) for 60 min, and then the activity was assayed according to the method in Section 2.4. The enzyme activity of *E. coli* BL21 (DE3)/pRSFDuet-1-*TLL-Cv*FAP at different pH values was determined using the method described in Section 2.4. The reaction buffers used were as follows: citrate-disodium hydrogen phosphate buffer (pH 4.0–5.0), phosphate buffer (pH 6.0–7.0), and Tris-HCl buffer (pH 8.0–9.0).

### 2.7. Scale-up experiment

The hydrolysis and photodecarboxylation of tripalmitin to pentadecane were scaled up from 1 ml to 100 ml. In this reaction, 2.0 g of tripalmitin and 100 ml of Tris-HCl buffer (pH 8.0, 100 $mmol \cdot L^{-1}$) containing 5.0 g of wet whole-cell *E. coli* BL21 (DE3)/pRSFDuet-1-*TLL-Cv*FAP were added to a transparent glass container. The container was added to the stir bar, sealed, and stirred gently (250 $r \cdot min^{-1}$) at 35 °C under blue light illumination overnight (36 h). The final reaction conditions of this reaction were as follows: [tripalmitin] = 24.77 $mmol \cdot L^{-1}$, [wet whole-cell *E. coli* BL21 (DE3)/pRSFDuet-1-*TLL-Cv*FAP] = 0.0500 $g \cdot ml^{-1}$, 35 °C. The product detection was the same as described above.

## 3. Results and Discussion

### 3.1. Enzyme selection for the coexpression system

Although *Cv*FAP is the first reported photodecarboxylase (FAP) that enables the decarboxylation of fatty acids into the corresponding $C_1$-shortened alkanes [13,14], our previous studies have characterized another 5 FAPs (*Cs*FAP, *Csi*FAP, *Gp*FAP, *Ng*FAP, and *Vc*FAP; see Table S1 for details) as having the same decarboxylation activities [16]. Along with the potentially broad availability of photodecarboxylases beyond green microalgae [15], there is a question regarding which FAP could best match lipases in cascade reactions. In addition, the catalytic activity, stability, and substrate scope of known FAPs are generally not comparable to those of lipases. The better the combination of lipase and photodecarboxylase, the higher the efficiency of the cascade reactions that can be obtained. Therefore, we started our investigation by screening different lipases and photodecarboxylases for the cascade reactions transforming tripalmitin (**1**) into pentadecane (**3**) (Fig. 1(a)). The lipases catalyzed the hydrolysis of tripalmitin (**1**) to generate free palmitic acid (**2**), which was subsequently decarboxylated into pentadecane (**3**).

Seven FAP genes (*Cs*FAP, *Csi*FAP, *Gp*FAP, *Ng*FAP, *Vc*FAP, *Cv*FAP, and its homolog *Cr*FAP) were heterologously expressed in *E. coli* BL21 (DE3), and the obtained cell-free extracts prepared from *E.* coli cells after simple ultrasonic treatment were used for cascade reactions. Concerning lipases, most of the widely reported lipases of fungal and yeast origin are not efficiently expressed in *E. coli* [22–25]. A lipase from *Thermomyces lanuginosus lipase* (*TL*L) has been proven to be overexpressed and active in *E. coli* [18,26]. Therefore, recombinant *TL*L was used for the screening of FAPs in cascade reactions. All reactions were performed with 5 $mmol \cdot L^{-1}$ tripalmitin (**1**), 0.15 $g \cdot ml^{-1}$ FAPs, and 0.05 $g \cdot ml^{-1}$ *TL*L under blue light illumination for 24 h, following the standard reaction conditions previously reported in the Ref. [8].

The results are summarized in Fig. 1. Gratifyingly, in each case, the substrate tripalmitin (**1**) was transformed into the desired pentadecane (**3**), with *Cv*FAP exhibiting the best production. Encouraged by these results, *Cv*FAP and *TL*L were chosen as representative fatty acid photodecarboxylase and lipase, respectively, to construct the coexpression system in the following part.

### 3.2. Design and construction of the coexpression system

We aim to develop cascade reactions (Fig. 1(a)) following a "whole-cell approach" in which a single *E. coli* BL21 (DE3) cell is made to express *Cv*FAP and *TL*L. Although attractive in principle, the approach can encounter limitations when efficient overall flux necessitates precise balancing between *Cv*FAP and *TL*L enzyme

(a)

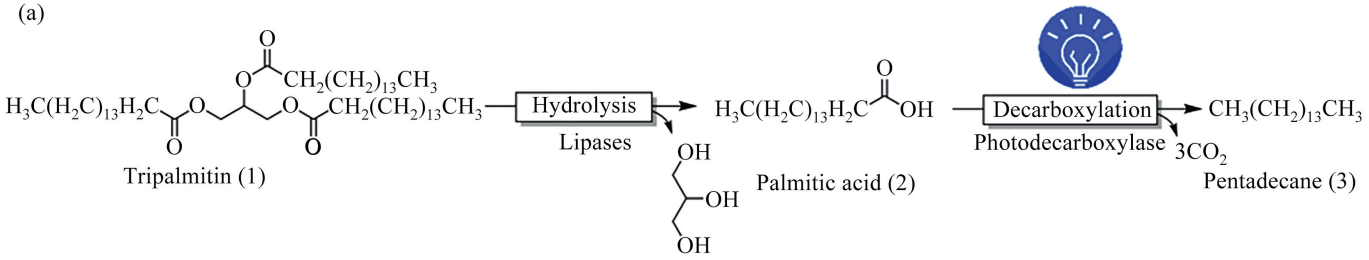


(b)

| Entry | FAP@whole cel (wet mass) | | Lipase | Substrate (tripalmitin) | Conversion |
|---|---|---|---|---|---|
| 1 | *Cv*FAP | 0.30 g | 100 mg | 24.77 mmol·L$^{-1}$ | 48.43% |
| 2 | *Cr*FAP | | | | 6.50% |
| 3 | *Csi*FAP | | | | 16.20% |
| 4 | *Cs*FAP | | | | 17.18% |
| 5 | *Gp*FAP | | | | 29.25% |
| 6 | *Ng*FAP | | | | 29.60% |
| 7 | *Vc*FAP | | | | 25.65% |

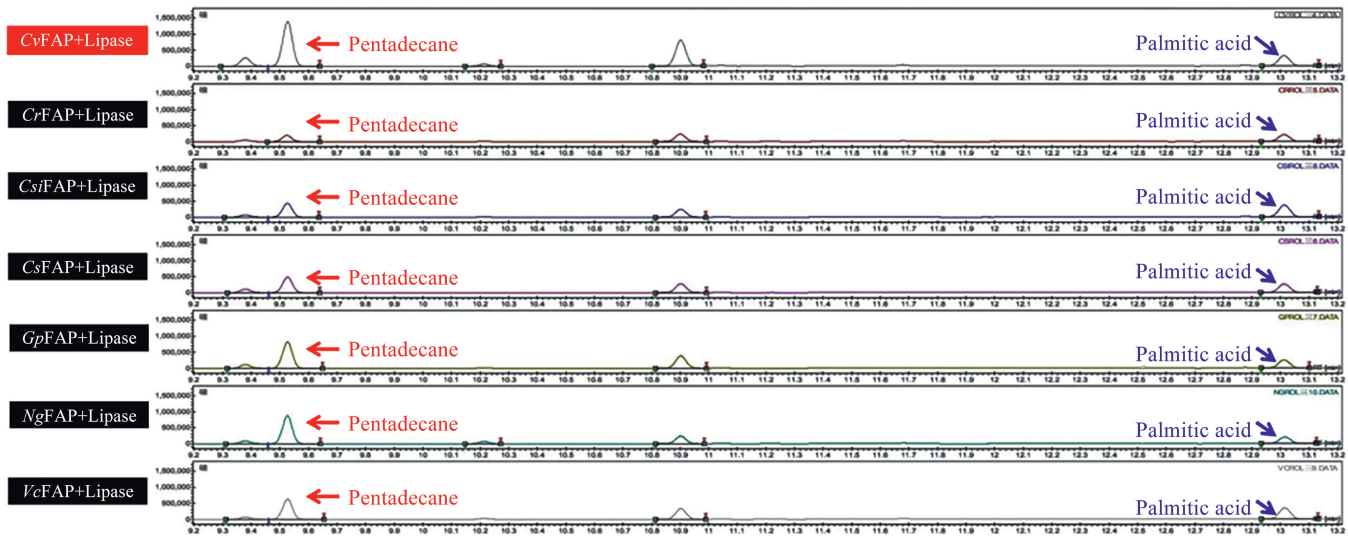


**Fig. 1.** The cascade reaction transforming tripalmitin (**1**) to pentadecane (**2**) by combining lipases and photodecarboxylases is a) the reaction scheme; b) the results of the combination of different FAPs with lipase *TL*L. The pentadecane standard and palmitic acid standard are shown in Fig. S2.

activities. Therefore, different single plasmid coexpression strategies were used to achieve the coexpression of *Cv*FAP and *TL*L in *E. coli* BL21 (DE3). (1) Based on the commercial Duet vectors pACYCDuet-1 and pRSFDuet-1, which have two biased cloning/expression regions containing two T7 promoters and one T7 terminator. For such vectors, the gene cloned downstream of the second promoter typically exhibits higher expression intensity, which is attributed to the absence of a terminator following the first promoter. *Cv*FAP and *TL*L were cloned into the first and second multiple cloning site (MCS) of these two dual promoter plasmids, respectively, to construct pACYCDuet-*TL*L-*Cv*FAP (named as "*E. Coli* BL21 (DE3)/pACY-*TL*L-*Cv*FAP") and pRSFDuet-*TL*L-*Cv*FAP (named "*E. Coli* BL21 (DE3)/pRSF-*TL*L-*Cv*FAP") (Fig. S1(a)). (2) Based on the pET28a(+) backbone, pET28a(+) is a single promoter plasmid itself, and we introduced a second T7 promoter by homologous recombination to construct pET28a(DualTer)-*TL*L-*Cv*FAP (named "*E. Coli* BL21 (DE3)/Double T7P *Cv*FAP-*TL*L") (Fig. S1(b)). The Double T7P *Cv*FAP-*TL*L coexpression plasmid is characterized by having two terminators in its expression structure, so both genes can be expressed under an identical framework. (3) Polycistronic coexpression strategy based on the pET-28a plasmid: The polycistronic coexpression strategy enables the simultaneous translation of two distinct enzyme proteins from a single mRNA by the incorporation of an additional ribosome binding site. The pET28a-*Cv*FAP-SD-*TL*L (named as "*E. Coli* BL21 (DE3)/SD-*Cv*FAP-*TL*L") polycistronic coexpression plasmid was constructed by the introduction of the Shine–Dalgarno (SD) sequence under one T7 promoter. As shown in Fig. S1(c), the main difference from the other two methods is that *Cv*FAP was constructed in the opposite position to *TL*L.

The constructed coexpression strains were induced to express *Cv*FAP and *TL*L activities under the same conditions as described in Sections 2.2 and 2.3. All four coexpression strains successfully

achieved the coexpression of the dual enzymes (*E. Coli* BL21 (DE3)/pRSF-*TLL*-*Cv*FAP, *E. Coli* BL21 (DE3)/pACY-*Cv*FAP-*TLL*, *E. Coli* BL21 (DE3)/Double T7P-*Cv*FAP-*TLL*, and *E. Coli* BL21 (DE3)/SD-*Cv*FAP-*TLL*). That is, each case resulted in soluble expression, although protein expression levels varied greatly among the strains. Sodium dodecyl-sulfate polyacrylamide gel *electrophoresis* (SDS–PAGE) analysis (Fig. 2) revealed two single bands with apparent molecular sizes of 83.3 and 31.6 kDa corresponding to the enzymes *Cv*FAP and *TLL*, respectively, confirming the theoretically calculated molecular mass (81.3 and 31.8 kDa) derived from the amino acid sequence. It must be mentioned that the structure of the expression framework varies among plasmid vectors, and the construction of different coexpression strategies using the same vectors can also lead to differences in molecular mass. Obviously, the coexpression of *E. coli* BL21 (DE3)/pRSF-*Cv*FAP-*TLL* and *E. coli* BL21 (DE3)/pACY-*Cv*FAP-*TLL* showed much better expression compared to that of *E. coli* BL21 (DE3)/Double T7P-*Cv*FAP-*TLL* and *E. coli* BL21 (DE3)/SD-*Cv*FAP-*TLL*. It must be emphasized that the coexpression *E. coli* BL21 (DE3)/pRSF-*Cv*FAP-*TLL* plasmid is distinguished from *E. coli* BL21 (DE3)/pACY-*Cv*FAP-*TLL* in terms of replications and resistance of the vectors. A closer look at the protein expression of enzyme activity levels indicates that for the dual enzyme coexpression system in this study, the copy number and resistance of the vector affect the amount of enzyme protein expression. Thus, compared to *E. Coli* BL21 (DE3)/pACY-*Cv*FAP-*TLL*, *E. coli* BL21 (DE3)/pRSF-*Cv*FAP-*TLL* performance was more in line with our needs.

Furthermore, studies concerning their catalytic activity using tripalmitin (**1**) as a standard substrate yielding pentadecane (**3**) revealed that *E. coli* BL21 (DE3)/pRSF-*Cv*FAP-*TLL* enabled a superior hydrolysis-decarboxylation performance compared to the other three dual enzymes (Fig. 3). It is worth mentioning that background reactions were performed in parallel with experiments of *E. coli* cells containing an empty vector as catalysts, no coexpression *E. coli* cells, and heat-denatured coexpression *E. coli* cells. No background reaction was taking place, indicating that the hydrolysis and decarboxylation reactions were affected by the active *TLL* and *Cv*FAP enzymes. A pattern can be drawn after comparing the catalytic activity and protein expression of the coexpression strains *E. coli* BL21 (DE3)/pACY-*Cv*FAP-*TLL*, *E. coli* BL21 (DE3)/pRSF-*Cv*FAP-*TLL*, *E. coli* BL21 (DE3)/Double T7P *Cv*FAP-*TLL*, and *E. coli* BL21 (DE3)/SD-*Cv*FAP-*TLL*.

The coexpression profile of the multiple *cis-trans* strategy construct is more complex. Both *Cv*FAP and *TLL* have differentially reduced expression, a phenomenon that may be caused by incomplete transcription of the second gene [27].

Based on the above results, we selected *E. coli* BL21 (DE3)/pRSF-*Cv*FAP-*TLL* as the subject for further study. In the first trial, the effect of substrate concentration on enzyme activities was investigated by using tripalmitin as the substrate to determine the optimal reaction conditions. The results are summarized in Fig. 4. When the substrate concentration reached 24.77 mmol·L$^{-1}$ (20 mg), *E. coli* BL21 (DE3)/pRSF-*Cv*FAP-*TLL* showed better catalytic activity to give 24.01 mmol·L$^{-1}$ of the desired product. An increase in the cell concentration of *E. coli* BL21 (DE3)/pRSF-*Cv*FAP-*TLL* from 0.0500 g·ml$^{-1}$ to 0.400 g·ml$^{-1}$ resulted in no significant change in the conversion. In the next attempt, the rotation speed was increased from 150 rpm to 250 r·min$^{-1}$ (300 r·min$^{-1}$, leading to the loss of enzyme activity). This revealed a significant increase in product formation when increasing the cell concentrations from 0.0500 g·ml$^{-1}$ to 0.300 g·ml$^{-1}$. When increasing the cell concentration above 0.400 g·ml$^{-1}$, no significant

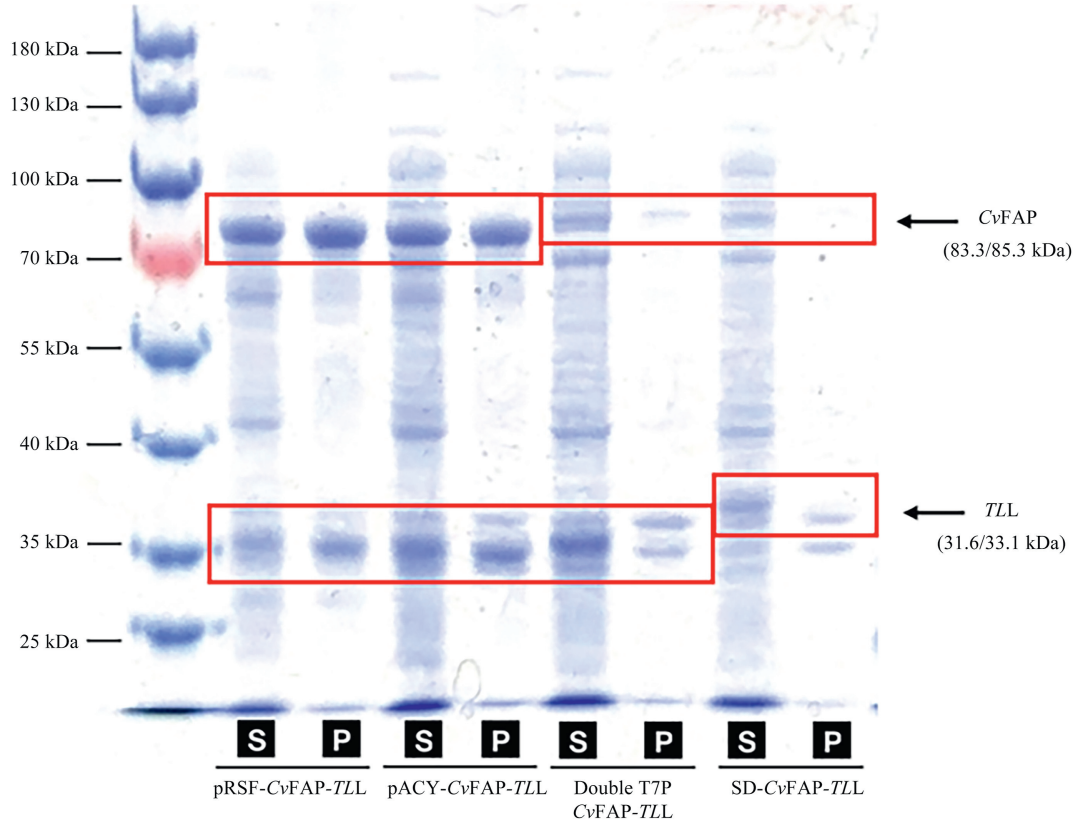


**Fig. 2.** SDS–PAGE analysis of the overexpression level of the coexpression plasmids pRSF-*Cv*FAP-*TLL*, pACY-*Cv*FAP-*TLL*, double T7P-*Cv*FAP-*TLL*, and SD-*Cv*FAP-*TLL* in *E. coli*, respectively. (Lane S: soluble fraction, Lane P: insoluble fraction.)

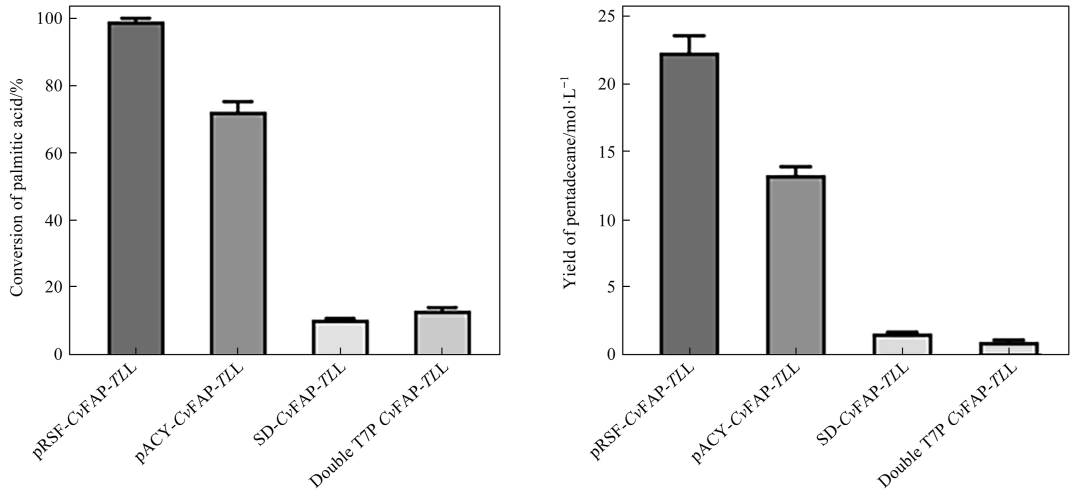


**Fig. 3.** Characterization of the tagged coexpression system, transforming tripalmitin (**1**) to yield pentadecane (**3**). (a) The conversion of pentadecane corresponding to palmitic acid (13 mmol·L$^{-1}$) as substrate; (b) the yield of pentadecane was obtained by using triglyceride tripalmitate as substrate (24.77 mmol·L$^{-1}$).

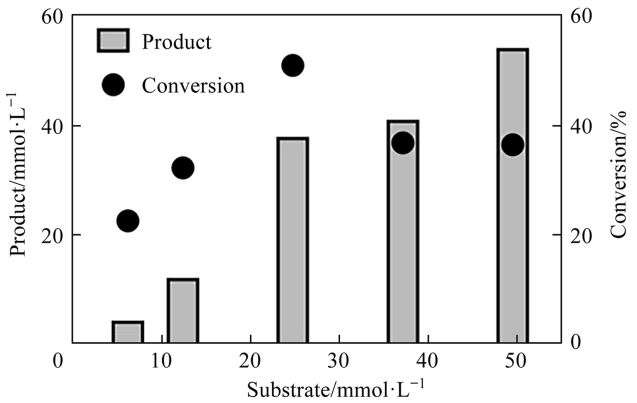


**Fig. 4.** Biotransformation of tripalmitin by whole cells of strain *E.coli* BL21 (DE3)/pRSFDuet-1-*TLL*-*Cv*FAP at different substrate concentrations

change in the conversion is observed. Therefore, it can be speculated that the reaction system might reach equilibrium between the addition of enzymes and the substrate concentrations. In a set of control experiments, no product formation was observed in the absence of *E. coli* BL21 (DE3)/pRSF-*Cv*FAP-*TLL* or in the absence of light illumination. Thus, the reactions are performed by the active enzymes (*Cv*FAP and *TLL*).

Reis *et al.* [28] demonstrated that Sn-2 monoglyceride, generated by the Sn-1, 3 regiospecific lipase, efficiently expelled the enzyme from the interface, leading to product inhibition. With further study, Muth *et al.* [29] proposed that the molar ratios between surfactants and lipase may eventually change the situation and lead to desorption of the lipase, leading to a halting of the catalytic reaction. Previous research has shown that the hydrolysis of tripalmitin might have difficulty achieving maximum product conversion without additional assistance; this also explains the low amount of final cascade catalytic products of tripalmitin found in our experiments above. It needs to be mentioned that we have investigated the rate-limiting step in such a coexpression whole-cell catalyst by adding an extra amount of *TLL*/*Cv*FAP into the reaction system, respectively (Table S4). A significant increase in the final product formation was observed when adding an extra amount of *Cv*FAP to the reaction system, which revealed that the decarboxylation of free fatty acids is the rate-limiting step. That is, the decarboxylation of free fatty acids efficiency may not catch up with the hydrolysis of oil. Protein engineering might be a solution to improve the decarboxylation of free fatty acids efficiency, which is currently being studied in our laboratory.

### *3.3. Optimization of the biotransformation conditions by whole cells of strain E. coli BL21 (DE3)/pRSF-chlorella variabilis NC64A-thermomyces lanuginosus lipase*

To fully assess the potential of *E. coli* BL21 (DE3)/pRSF-*Cv*FAP-*TLL* in transforming tripalmitin (**1**) to pentadecane (**3**), in the next step, we further optimized the cascade reaction conditions. The influence of pH on the enzyme activities was investigated by monitoring the change in enzyme activity toward tripalmitin (Fig. 5(a)). The activity-pH profile of the enzymes gave a broad peak over the range of pH 5.0–8.0. However, the coexpressed enzyme showed poor activity at pH below 5.0 or pH above 9.0, which was attributed to the poor pH tolerance of the intrinsic enzymatic properties of *Cv*FAP. The optimal activity was observed at pH 8.0 in potassium phosphate buffer. In previous work, characterization of *Cv*FAP indicated that its activity was optimum at approximately pH 8.5, while *TLL* had a broad activity-pH profile over the range of pH 7.0–12.0 [14,30]. Studies concerning thermostability were performed at different temperatures from 30 to 70 °C (Fig. 5(b)). Not surprisingly, the results show that the whole cells of strain *E. coli* BL21 (DE3)/pRSF-*Cv*FAP-*TLL* is relatively stable at 50 °C but lose their activity almost completely after incubation at 60 °C for 1 h. Moreover, the enzyme is stable at 40 °C for 1 h without any activity loss, which is consistent with previous reports. *Cv*FAP activity begins to decline sharply when the temperature exceeds 40 °C [31], while a decline in *TLL* activity occurs at 60 °C [32], which clearly explains the results presented in Fig. 5(b). Thus, the activity of *E. coli* BL21 (DE3)/pRSFDuet-*Cv*FAP-*TLL* enzymes attained its maximum at 30–40 °C as well as pH 8.0.

To investigate more factors affecting the hydrolytic decarboxylation reaction of tripalmitin (**1**), we monitored the time course at 35 °C and pH 8.0 for 72 h. The reaction with 0.05 g·ml$^{-1}$ cells gave a maximum yield of 24.77 mmol·L$^{-1}$ of the desired pentadecane (**3**) after 24 h, and even after a prolonged reaction time, no increase in yield was observed (Fig. 6). Based on the widely reported stability of *TLL*, the shortcoming of the catalytic activity of the coexpression system remains *Cv*FAP.

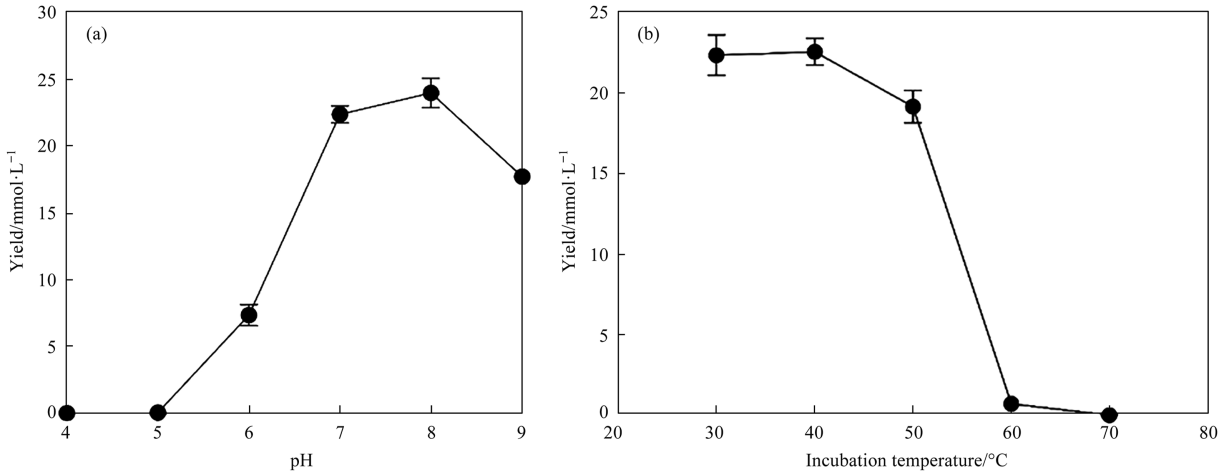


**Fig. 5.** pH profile and thermostability (incubation at given temperatures for 1 h) of whole cells of strain *E.coli* BL21 (DE3)/pRSF-*TLL-Cv*FAP for the hydrolysis and decarboxylation activities. Reaction conditions: reaction volume: 1 ml in total, 50 μl oil, 950 μl Tris-HCl buffer (pH 8.0, 100 mmol·L$^{-1}$), 37 °C, 150 r·min$^{-1}$, 36 h.

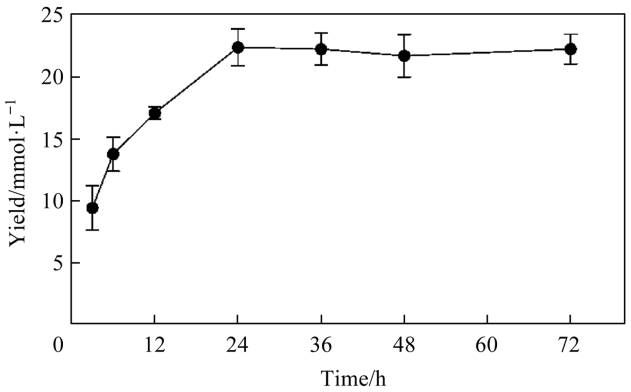


**Fig. 6.** Time course of hydrolysis and photodecarboxylation of tripalmitin (**1**) by *E. coli* BL21 (DE3)/pRSF-*TLL-Cv*FAP

### *3.4. The use of a coexpression system for alkane production from natural oils*

2To demonstrate the applicability of the proposed coexpression system hydrolysis/decarboxylation cascade reactions, we explored the substrate scope and broadened the substrate range to various natural oils. In total, seven commercially available oils were evaluated (Table 1). As expected, most of the oils evaluated were converted into the corresponding saturated alkanes with a product concentration of 4.86–15.83 mmol·L$^{-1}$. It is worth mentioning that the overall concentrations and compositions of fatty acids vary from different types of vegetable oils, leading to the different production of alkanes. Especially corn oil gave poor conversion, which most likely can be attributed to its carboxylic acid composition consisting of more than 85% of $C_{12}$ and shorter carboxylic acids. These shorter carboxylic acids are rather poor substrates for *Cv*FAP, thereby rationalizing the poorer alkane yield in this case. Besides, the obtained results are consistent with previous studies [8] that the highest abundance

**Table 1**
Hydrolyzed photodecarboxylated natural oils to obtain saturated alkanes

| Entry | Natural oil | Fatty acid | Alkane | Product/mmol·L$^{-1}$ | Total product/mmol·L$^{-1}$ | Conversion rate /mmol·L$^{-1}$·h$^{-1}$·g$^{-1}$ |
|---|---|---|---|---|---|---|
| 1 | Palm oil | Palmitic acid ($C_{16}$) | Pentadecane ($C_{15}$) | 10.22 | 15.38 | 8.33 |
| | | Stearic acid ($C_{18}$) | Heptadecane ($C_{17}$) | 5.16 | | |
| 2 | Peanut oil | Palmitic acid ($C_{16}$) | Pentadecane ($C_{15}$) | 3.26 | 8.06 | 4.48 |
| | | Stearic acid ($C_{18}$) | Heptadecane ($C_{17}$) | 4.8 | | |
| 3 | Olive oil | Palmitic acid ($C_{16}$) | Pentadecane ($C_{15}$) | 2.27 | 6.13 | 3.41 |
| | | Stearic acid ($C_{18}$) | Heptadecane ($C_{17}$) | 3.86 | | |
| 4 | Rice bran oil | Palmitic acid ($C_{16}$) | Pentadecane ($C_{15}$) | 3.61 | 5.94 | 3.30 |
| | | Stearic acid ($C_{18}$) | Heptadecane ($C_{17}$) | 2.33 | | |
| 5 | Cottonseed oil | Palmitic acid ($C_{16}$) | Pentadecane ($C_{15}$) | 2.53 | 8.35 | 4.64 |
| | | Stearic acid ($C_{18}$) | Heptadecane ($C_{17}$) | 5.82 | | |
| 6 | Linseed oil | Palmitic acid ($C_{16}$) | Pentadecane ($C_{15}$) | 2.77 | 8.59 | 4.77 |
| | | Stearic acid ($C_{18}$) | Heptadecane ($C_{17}$) | 5.82 | | |
| 7 | Corn oil | Palmitic acid ($C_{16}$) | Pentadecane ($C_{15}$) | 2.51 | 4.86 | 2.70 |
| | | Stearic acid ($C_{18}$) | Heptadecane ($C_{17}$) | 2.35 | | |
| 8 | Soybean oil | Palmitic acid ($C_{16}$) | Pentadecane ($C_{15}$) | 1.9 | 8.05 | 4.47 |
| | | Stearic acid ($C_{18}$) | Pentadecane ($C_{15}$) | 6.09 | | |

Note: Reaction conditions: 950 μl of Tris-HCl buffer (pH 8.0, 100 mmol·L$^{-1}$) containing 0.0500 g of *E. coli* BL21 (DE3)/pRSFDuet-1-*TLL-Cv*FAP and 50 μl of oil were added to a transparent glass vial (total reaction volume was 1 ml). The final conditions of this reaction were [*E. coli* BL21 (DE3)/pRSFDuet-1-*TLL-Cv*FAP] = 0.0500 g·ml$^{-1}$, [Oil] = 50 μl·ml$^{-1}$, exposed under blue light for 36 h.

The yields of products were quantified by GC using a calibration line. Experiments were performed in triplicate, and the average values were shown as the final results.

of fatty acid feedstocks containing $C_{16}$ and $C_{18}$ chain lengths is found in natural oils and fats. The same is true that the saturated alkanes ($C_{15}$, $C_{17}$) of the products are found as the main products. This implies that this concept may have the potential to serve as a reliable fermentation source for a specific chain-long alkane production mode.

Furthermore, when compared to the results of coexpression whole-cell catalysts with those reported in the previous studies on biofuel production *via* catalysis of lipase and photodecarboxylase [33,34], it was found that such coexpression whole-cell catalysts resulted in product (hydrocarbon fuel) formation with good to excellent concentrations. For example, Karava and co-workers [33] developed a *Bacillus subtilis* spore display platform for lipase and fatty acid photodecarboxylase and used the bienzymatic one-pot cascade for the production of hydrocarbons. Although the technology benefits from its simplicity, the overall yields were very poor (a product concentration of 0.7 mmol·$L^{-1}$ corresponding to 3.5% conversion was observed). The group of Liao [34] provided a cascade system integrating lipase hydrolysis and *Cv*FAP decarboxylation for continuous hydrocarbon fuels. It is worth mentioning that in such a cascade system, various oils can be converted to hydrocarbon fuels with a concentration of 8.97–15.3 mmol·$L^{-1}$, corresponding to an optimal conversion of 61.2%. However, the use of purified lipase, a crude enzyme solution of *Cv*FAP, and the microfluidic photobioreactor led to an extra energy input.

After performing experiments on a small scale to further our understanding of the behavior of enzymes under various conditions, we found that the desired product, pentadecane, could be obtained with a maximum concentration of 24.01 mmol·$L^{-1}$ when 24.77 mmol·$L^{-1}$ tripalmitin was loaded. Hence, we tested the scalability of the developed reaction system. The biotransformation of tripalmitin to alkane was scaled up from 1 ml to 100 ml using resting cells of *E. coli* BL21 (DE3)/pRSFDuet-1-*TL*L-*Cv*FAP. to give the desired pentadecane in a yield of 18.89 mmol·$L^{-1}$, which falls short of expectations due to the *in-situ* production of highly surface-active intermediates, which inhibited further enzymatic conversion [35].

## 4. Conclusions

In this study, an engineered strain of *E. coli* containing a lipase (*TL*L) and a fatty acid photodecarboxylase (*Cv*FAP) was constructed for the first time to produce alkane-based biofuels from natural oils. In brief, double-free enzyme catalysis was performed using 7 FAPs from different sources with lipase *TL*L. Four coexpression systems were established based on three distinct single-plasmid co-expression strategies, and the optimal combination of *E. coli* BL21 (DE3)/pRSF-*Cv*FAP-*TL*L was obtained. In follow-up transformation reactions with tripalmitin as a standard substrate, *E. coli* BL21 (DE3)/pRSFDuet-1-*TL*L-*Cv*FAP cells enabled a superior hydrolytic-decarboxylation performance. Under the optimized conditions, the *TL*L-*Cv*FAP coexpression system readily hydrolyzed and decarboxylated a series of natural oils into the corresponding alkanes under blue light illumination. The desired product (24.01 mmol·$L^{-1}$) was achieved using 24.77 mmol·$L^{-1}$ natural oils as the substrate. Scaling up the reaction to 100 ml also yielded 18.89 mmol·$L^{-1}$ of product. The thermal stability study indicates that the coexpression system is capable of being applied in a reaction below 50 °C. Our results suggested that lipase and photodecarboxylase were compatible and that the properties characterized by the coexpression system were superimposed on the properties of the individual enzymes. This work contributes to the development of a new catalytic method for the environmentally benign and scalable synthesis of biofuels from renewable starting materials.

## Data Availability

No data was used for the research described in the article.

## Declaration of Interest

The authors declare that they have no known competing financial interests or personal relationships that could have appeared to influence the work reported in this paper.

## Acknowledgements

The work was financially supported by the National Natural Science Foundation of China (42376097); Guangdong Basic and Applied Basic Research Foundation (2023A1515030226, 2021A1515010829).

## Supplementary Material

Supplementary data to this article can be found online at https://doi.org/10.1016/j.cjche.2023.11.013.

## References

[1] N.Z. Abdul Kapor, G.P. Maniam, M.H.A. Rahim, M.M. Yusoff, Palm fatty acid distillate as a potential source for biodiesel production-A review, *J. Clean. Prod.* 143 (2017) 1–9.
[2] I. Riaz, I. Shafiq, F. Jamil, A. Al-Muhtaseb, P. Akhter, S. Shafique, Y. Park, M. Hussain, A review on catalysts of biodiesel (methyl esters) production, *Catal. Rev. Sci. Eng.* (2022), https://doi.org/10.1080/01614940.2022.2108197.
[3] A. Kumar, V.P. Singh, A. Srivastava, Quality biodiesel *via* biotransesterification from inedible renewable sources, *J. Clean. Prod.* 379 (2022) 134653.
[4] P. Kharia, R. Saini, V.K. Kudapa, A study on various sources and technologies for production of biodiesel and its efficiency, *MRS Energy Sustain* 10 (1) (2023) 35–51.
[5] N. Tien Thanh, M. Mostapha, M.K. Lam, S. Ishak, Y. Kanna Dasan, J.W. Lim, I.S. Tan, S.Y. Lau, B.L.F. Chin, T. Hadibarata, Fundamental understanding of *in-situ* transesterification of microalgae biomass to biodiesel: A critical review, *Energy Convers. Manag.* 270 (2022) 116212.
[6] J.I. Orege, O. Oderinde, G.A. Kifle, A.A. Ibikunle, S.A. Raheem, O. Ejeromedoghene, E.S. Okeke, O.M. Olukowi, O.B. Orege, E.O. Fagbohun, T.O. Ogundipe, E.P. Avor, O.O. Ajayi, M.O. Daramola, Recent advances in heterogeneous catalysis for green biodiesel production by transesterification, *Energy Convers. Manag.* 258 (2022) 115406.
[7] M.M.E. Huijbers, W.Y. Zhang, F. Tonin, F. Hollmann, Light-driven enzymatic decarboxylation of fatty acids, *Angew. Chem. Int. Ed.* 57 (41) (2018) 13648–13651.
[8] Y.J. Ma, X.Z. Zhang, W.Y. Zhang, P.L. Li, Y.R. Li, F. Hollmann, Y.H. Wang, Photoenzymatic production of next generation biofuels from natural triglycerides combining a hydrolase and a photodecarboxylase, *ChemPhotoChem* 4 (1) (2020) 39–44.
[9] E.F. Aransiola, T.V. Ojumu, O.O. Oyekola, T.F. Madzimbamuto, D.I.O. Ikhu-Omoregbe, A review of current technology for biodiesel production: State of the art, *Biomass Bioenergy* 61 (2014) 276–297.
[10] J.S. Huang, Y.M. Jian, P. Zhu, O. Abdelaziz, H. Li, Research progress on the photo-driven catalytic production of biodiesel, *Front. Chem.* 10 (2022) 904251.
[11] Z.P. Huang, Z.T. Zhao, C.F. Zhang, J.M. Lu, H.F. Liu, N.C. Luo, J. Zhang, F. Wang, Enhanced photocatalytic alkane production from fatty acid decarboxylation *via* inhibition of radical oligomerization, *Nat. Catal.* 3 (2) (2020) 170–178.
[12] B.S. Chen, Y.Y. Zeng, L. Liu, L. Chen, P.G. Duan, R. Luque, R. Ge, W.Y. Zhang, Advances in catalytic decarboxylation of bioderived fatty acids to diesel-range alkanes, *Renew. Sustain. Energy Rev.* 158 (2022) 112178.
[13] D. Sorigué, K. Hadjidemetriou, S. Blangy, G. Gotthard, A. Bonvalet, N. Coquelle, P. Samire, A. Aleksandrov, L. Antonucci, A. Benachir, S. Boutet, M. Byrdin, M. Cammarata, S. Carbajo, S. Cuiné, R.B. Doak, L. Foucar, A. Gorel, M. Grünbein, E. Hartmann, R. Hienerwadel, M. Hilpert, M. Kloos, T.J. Lane, B. Légeret, P. Legrand, Y. Li-Beisson, S.L.Y. Moulin, D. Nurizzo, G. Peltier, G. Schirò, R.L. Shoeman, M. Sliwa, X. Solinas, B. Zhuang, T.R.M. Barends, J.P. Colletier, M. Joffre, A. Royant, C. Berthomieu, M. Weik, T. Domratcheva, K. Brettel, M.H. Vos, I. Schlichting, P. Arnoux, P. Müller, F. Beisson, Mechanism and dynamics of fatty acid photodecarboxylase, *Science* 372 (6538) (2021) eabd5687.
[14] D. Sorigué, B. Légeret, S. Cuiné, S. Blangy, S. Moulin, E. Billon, P. Richaud, S. Brugière, Y. Couté, D. Nurizzo, P. Müller, K. Brettel, D. Pignol, P. Arnoux, Y. Li-Beisson, G. Peltier, F. Beisson, An algal photoenzyme converts fatty acids to hydrocarbons, *Science* 357 (6354) (2017) 903–907.
[15] S.L.Y. Moulin, A. Beyly-Adriano, S. Cuiné, S. Blangy, B. Légeret, M. Floriani, A. Burlacot, D. Sorigué, P.P. Samire, Y. Li-Beisson, G. Peltier, F. Beisson, Fatty acid

photodecarboxylase is an ancient photoenzyme that forms hydrocarbons in the thylakoids of algae, *Plant Physiol* 186 (3) (2021) 1455–1472.
[16] Y.Y. Zeng, X.J. Yin, L. Liu, W.Y. Zhang, B.S. Chen, Comparative characterization and physiological function of putative fatty acid photodecarboxylases, *Mol. Catal.* 532 (2022) 112717.
[17] W. Zhang, M. Ma, M.M.E. Huijbers, G.A. Filonenko, E.A. Pidko, M. van Schie, S. de Boer, B.O. Burek, J.Z. Bloh, W.J.H. van Berkel, W.A. Smith, F. Hollmann, Hydrocarbon synthesis *via* photoenzymatic decarboxylation of carboxylic acids, *J. Am. Chem. Soc.* 141 (7) (2019) 3116–3120.
[18] X.R. Zhong, Y.J. Ma, X.Z. Zhang, J.H. Zhang, B. Wu, F. Hollmann, Y.H. Wang, More efficient enzymatic cascade reactions by spatially confining enzymes *via* the SpyTag/SpyCatcher technology, *Mol. Catal.* 521 (2022) 112188.
[19] F.S. Aalbers, M.W. Fraaije, Enzyme fusions in biocatalysis: Coupling reactions by pairing enzymes, *Chembiochem* 20 (1) (2019) 20–28.
[20] Z. Wang, Y. Zhou, X.Y. Ren, K. Wei, X.L. Fan, L.C. Huang, D.S. Zhao, L. Zhang, C. Q. Zhang, Q.Q. Liu, Q.F. Li, Co-overexpression of two key source genes, *OsBMY4* and *OsISA3*, improves multiple key traits of rice seeds, *J. Agric. Food Chem.* 71 (1) (2023) 615–625.
[21] X.L. Xiang, B.H. Hu, Z.G. Pu, L.Y. Wang, T. Leustek, C.S. Li, Co-overexpression of *AtSAT1* and *EcPAPR* improves seed nutritional value in maize, *Front. Plant Sci.* 13 (2022) 969763.
[22] M. Di Lorenzo, A. Hidalgo, M. Haas, U.T. Bornscheuer, Heterologous production of functional forms of *Rhizopus oryzae* lipase in *Escherichia coli*, *Appl. Environ. Microbiol.* 71 (12) (2005) 8974–8977.
[23] M. Tian, J. Zhang, W. Luo, Z.Y. Wang, J.Y. Fu, S.W. Huang, P.M. Lü, Propeptide-mediated protein folding: mechanism and its impact on lipase, *Sheng Wu Gong Cheng Xue Bao* 37 (1) (2021) 88–99. (in Chinese)
[24] H.D. Beer, G. Wohlfahrt, R.D. Schmid, J.E. McCarthy, The folding and activity of the extracellular lipase of *Rhizopus oryzae* are modulated by a prosequence, *Biochem. J.* 319 (Pt 2) (1996) 351–359.
[25] H.D. Beer, J.E. McCarthy, U.T. Bornscheuer, R.D. Schmid, Cloning, expression, characterization and role of the leader sequence of a lipase from *Rhizopus oryzae*, *Biochim. Biophys. Acta* 1399 (2–3) (1998) 173–180.
[26] R. Fernandez-Lafuente, Lipase from *Thermomyces lanuginosus*: Uses and prospects as an industrial biocatalyst, *J. Mol. Catal. B* 62 (3–4) (2010) 197–212.
[27] R. Ma, H. Xu, R. Ding, Multigene co-expression strategies of *Escherichia coli*, *China Biotech* 32 (2012) 117–122.
[28] P. Reis, R. Miller, M. Leser, H. Watzke, V.B. Fainerman, K. Holmberg, Adsorption of polar lipids at the water-oil interface, *Langmuir* 24 (11) (2008) 5781–5786.
[29] M. Muth, S. Rothkötter, S. Paprosch, R.P. Schmid, K. Schnitzlein, Competition of *Thermomyces lanuginosus* lipase with its hydrolysis products at the oil-water interface, *Colloids Surf. B Biointerfaces* 149 (2017) 280–287.
[30] E. Jurado, F. Camacho, G. Luzón, M. Fernández-Serrano, M. García-Román, Kinetics of the enzymatic hydrolysis of triglycerides in O/W emulsions, *Biochem. Eng. J.* 40 (3) (2008) 473–484.
[31] Y.Q. Wu, C.E. Paul, F. Hollmann, Stabilisation of the fatty acid decarboxylase from chlorella variabilis by caprylic acid, *Chembiochem* 22 (14) (2021) 2420–2423.
[32] E. Jurado, V. Bravo, J. Núñez-Olea, R. Bailón, D. Altmajer-Vaz, M. Garía-Román, A. Fernández-Arteaga, Enzyme-based detergent formulas for fatty soils and hard surfaces in a continuous-flow device, *J. Surfactants Deterg.* 9 (1) (2006) 83–90.
[33] M. Karava, P. Gockel, J. Kabisch, *Bacillus subtilis*spore surface display of photodecarboxylase for the transformation of lipids to hydrocarbons, *Sustain. Energy Fuels* 5 (6) (2021) 1727–1733.
[34] F. Li, A. Xia, X.B. Guo, W.Y. Zhang, Y. Huang, X.Q. Zhu, X. Zhu, Q. Liao, Continuous hydrocarbon fuels production by photoenzymatic decarboxylation of free fatty acids from waste oils, *J. Environ. Chem. Eng.* 11 (5) (2023) 110748.
[35] P. Reis, K. Holmberg, R. Miller, M.E. Leser, T. Raab, H.J. Watzke, Lipase reaction at interfaces as self-limiting processes, *Comptes Rendus Chim* 12 (1–2) (2009) 163–170.